Eng Int Syst (2025) 5: 545–553

Engineering
Intelligent Systems

High-precision Motion Capture System Based on 3D Space Animation Scene Construction Based on Optical Fiber Communication Network

Jiayi Li*

Department of Anime Arts, Zibo Polytechnic University, Zibo 255300, Shandong, China

Motion capture technology has advanced quickly in recent years thanks to the rapid development of sensor technology, the invention of inertial navigation, and the ongoing development of hardware configurations for measurement and computation. With the advancement of communication technology, optical fiber communication networks are now the most widely used form of communication, and they are fiercely competitive with other forms of communication. Consequently, the combination of a motion capture system and an optical fiber communication network offer several potential applications. For instance, the electronic optical motion capture technology and the virtual reality technology can be combined to produce a very realistic character animation effect in the creation of large-scale 3D games. Human motion capture technology is widely used in the film and television animation industry to make the characters more realistic. In this research, a high-precision motion capture system based on a three-dimensional space animation scenario using an optical fiber communication network is proposed. The system was built using the technology of the optical fiber communication network and motion capture. An experiment was conducted to determine the accuracy of the motion capture system. The experimental findings indicate that without a high-speed optical fiber in the time domain, the average motion capture accuracy was 46.7%. The addition of high-speed optical fiber time domain improved the average accuracy of the motion capture by 2.5%, and improved the performance of each joint point capture.

Keywords: motion capture system, optical fiber communication network, three-dimensional space, animation scene

1. INTRODUCTION

At present, the development of motion capture, whether by universities or companies, has reached a certain level due to comprehensive explorations of this field, and commercial products with relatively stable performance have appeared in the market. The motion capture operating system is a machine that records the real-time positioning of objects or people in motion, and is being widely used in many industries. Of the various motion capture methods, the ones utilizing an optical fiber communication network are more accurate and the most popular, Due to its advantages of high precision, instant data transmission and, simultaneously, more accurate measurement, in addition to traditional motion recovery for movie animation and other applications, in recent years, optical fiber communication network motion capture system software has also been used in industry and for purposes

*Address for correspondence: Jiayi Li, Department of Anime Arts, Zibo Polytechnic University, Zibo 255300, Shandong, China, Email: 12660@zbvc.edu.cn

such as the precise measurement of component installation points, laboratory development, the design of robot control mechanisms, and inspection.

Yang built a distributed real-time motion capture system based on Kinect in the most recent motion capture research. With calibration sticks, he determined the relative position of the Kinect v2 sensor using trigonometry and automatically saved the sensor's location. He found that the accuracy of motion capture can be increased by merging data from various sensors using nonlinear least squares [1]. Ganguly [2] compared finger kinematics data between a land mobile channel and the marker-based industry standard Qualisys Track Manager (QTM) motion capture system. According to this research, gold standard motion capture systems cannot be replaced by the present land mobile channels in clinical situations. However, in terms of updating and upgrading, additional research is required to confirm the functionality of the land mobile channel [2]. Schlage suggested employing a low-cost inertial measurement device-based development system to create a transportable, simple-to-use motion, and readily scalable capture system. The system can be adjusted to fit each body part with ease thanks to its modular architecture. Human motion sequences were collected and the three joint angles of the lower extremities were determined so as to detect misalignment; however, this was the main focus of this work [3]. In addition to proposing a mechanical model, Mrozek introduced the use of mobile communication motion capture systems to test and evaluate flexible manufacturing systems based on certain criteria. Motion capture devices and suitable biomechanical models provided a more objective evaluation of physical performance and the identification of any dysfunction of the examinee's motor systems [4].

Other researchers adopted different approaches. For instance, Rizaldy investigated the motion capture system's relative accuracy using action sport cameras (ASC). He tested the proposed ASC Mocap system using the well-known Vicon V8 with a 10-camera setup. He gathered gait information concurrently to ensure accurate comparisons. The ASC-based system was assessed by comparing the resulting spatiotemporal and kinematic characteristics with those obtained using Vicon [5]. Based on planar fiducial markers, Mostashiri designed a small, portable, inexpensive, and straightforward motion capture device. Accurate data for spatial jaw motion capture was provided by the motion capture system's sensor fusion of measurements from two webcams. Mostashiri investigated the capacity of motion capture systems to record both planar and spatial motion by simultaneously recording complex 3-D motions of human subject tangent points with motion capture systems and commercially available research-oriented optical motion capture systems [6]. Burger et al. combined the Qualisys Oqus optical motion capture technology with the Ergoneers Dikablis head-mounted eye tracker. At the beginning of each recording, the participant focuses on the target, and keeping their eyes open to synchronize the recordings from the two devices, gives a quick nod which produces a sharp vertical displacement in both mocap and eye data. A peak selecting technique can successfully identify this displacement and utilize it to match motion capture and ocular data [7]. An optical motion capture system with 18 OptiTrack Flex13 cameras and external reference points calibrated using measuring techniques was examined by Gn to determine its absolute volumetric accuracy. In addition to evaluating how the accuracy depends on the number of cameras, as indicated by the static detection noise in the marker coordinates, the absolute accuracy—expressed as the difference between the reference and measured coordinates—was also determined [8].

The advantage of the motion capture system based on the optical fiber communication network is that the equipment is not constrained by cables and mechanical systems. The marker points can be flexibly fixed on the participant's body, and the participant engages in a range of activities that can be performed at will. In addition, the capture system constructed by optical fiber communication network technology can also record certain positions that cannot be captured by other systems. Moreover, it can capture fast-moving targets. The operating scale of the system is adjustable, and the total number of marking points can be adjusted flexibly according to the actual operating position.

2. CONSTRUCTION METHOD OF HIGH-PRECISION MOTION CAPTURE SYSTEM

The high-precision motion capture system captures the double-beam marker points based on the infrared fiber optic lens for accurate three-dimensional coordinate measurement. The lens emits infrared rays around it. According to the captured refracted light, the data of the marked point is stored as a grayscale image, and the grayscale image is binarized. The position of the marker point in the two-dimensional image can be obtained from the number of pixels. As long as two lenses capture the same mark at the same time, the mark point in three-dimensional space can be reconstructed with the help of the basic principle of binocular vision. Different numbers of parameter lenses are established according to the size of the system website and the overall target capture area [9].

The lower computer and the higher computer software make up the high-precision motion capture system. The wireless module transfers the sensor node data to the PC in real time from the lower computer, which is a sensor node spread throughout the entire optical fiber communication network [10]. The PC is also utilized to run the top computer's software platform. The data of the cognitive node is immediately received via the external antenna. The software platform evaluates and interprets the data that has been received, and it quickly displays computer visuals that show the body posture [11].

The following functionalities and processing modules are necessary in order to ensure that the software system has the requisite performance and usability while also meeting the operating requirements of the high-precision motion capture system itself:

(1) Receive serial communication data

This is usually real-time detection of wireless network data received by electronic computer serial communication, instantly receiving data from key sensor nodes throughout our body. The sensor data connection points of each optical fiber communication system Internet are distinguished, and these data are sent to the control module for data preparation processing.

(2) Data preparation processing

The key is to achieve the power preparation processing of the initial signal, and to compensate and filter out any signal with deviation and noise. These data are divided into two parts: attitude measurement control module and real-time storage data.

(3) Analysis of human action posture

The optimization algorithm for human action and posture analysis depends on the results obtained from data preparatory processing, as well as the posture calculation and analysis of human actions.

(4) Carrying and operation of the mannequin

This involves the construction of the game model, introduces the system software 3D scenario, and uses the data to determine the human body posture calculated by the control module to capture the human body model in real time.

(5) Enhance the appearance of the software system

Part of this function involves skin replacement and the beautification of data visualization controls, menu bars, article titles, toolbars and other features. In the VC++ development tools, the visibility controls, toolbars and menu bars do not have corresponding enhancement functions, which can be set and produced by customization.

(6) Related auxiliary functions

If a person wants to peruse the camera data of the three-dimensional scene, they can choose a computer mouse or a keyboard to convert the angle and zoom in and out of the main view. Other 3D modeling can be established under the 3D scene to make it more three-dimensional [12–13].

According to the optical fiber network communication and the sensor structure of the optical device, the two main parameters, the bending angle of the index finger and the bending angle of the thumb around the index finger in the human posture, are tested to manipulate the high-precision capture system constructed by the three-dimensional space animation scene.

The plastic optical fiber is used to measure the bent angle of the index finger, and the bending sensitization countermeasure is implemented to make the plastic optical fiber more sensitive to the angle. If it is not sensitized, the loss of plastic optical fiber in transmission would be very weak. This sensitization measure is characterized by simple production and fabrication, and the sensor structure combines the advantages of the flexibility and miniaturization of optical fibers, and can be installed on human fingers [14].

The structural design of the angle sensor is intended to miniaturize the core components of the experimental design scheme of the computer mouse. LEDs and photodetectors in the form of small and medium packages are selected. The sensor structure can be worn on the hand to test the bending angle of the thumb around the index finger. The bending angle of the index finger can be accurately measured according to the bending angle of the correct guiding structure of the index finger by checking its bending angle [15].

The system's lower computer and top computer software communicate with one another through wireless data transmission and serial communication. Real-time monitoring of the serial communication port of the system's received data is required by VC++. In VC++, enabling the system software application program interface. Using external serial communication classes, and using serial communication controls that follow the component object model, are the ways that are typically used to receive serial communication data. The serial communication has good performance and can shield the complicated basic operations. The performance is stable and the software development cycle can be shortened. The software system uses ActiveX serial communication control MSCOMM. The serial communication control MSCOMM can perform thematic activity viewing mode and event-driven mode. Setting parameters like serial number, serial port baud rate, and input/export buffer size are part of the reset serial communication operation. Finally, the buffer area's data is pre-read, and any residual data is removed [16–17].

The serial connection interface has a very high data transfer rate. The data receiving component is packaged in a separate control module, and the system software runs concurrently and starts a new thread in the control module to prevent the data from being deposited and lost. Each thread in VC++ must descend from the member function class. There are two different types of threads: worker threads without thread pools, and functional interface threads with maintenance thread pools and information flow systems. The operation interface thread is used for interacting with the user and responding to the field input and events opened by the external computer operating system in real time. Instead of interacting with users, workers are used to solve computationally intensive tasks such as printer servicing and delivery. Using worker threads as receiver threads is a good option. Figure 1 shows the data reception flow chart. First, after creating an object operation, one can create a worker thread that does a serial communication port reset. This enables the ComEvent characteristic of the serial communication port and the receive mode of the serial communication port to be distinguished. Finally, it is determined whether or not the source program is completed, and the thread network resources are released [18].

The data frame format uploaded by the sensor node in the optical fiber communication network is depicted in Figure 2. The raw data of the sensor node in the frame can be parsed while loading the serial communication buffer data. The initial data is preserved as a document in a specific format while being transmitted to the attitude measurement control module, making it possible to further analyze and conduct scientific study on sensor node data offline [19].

The majority of the offline data that is typically collected for algorithm development, and it must be kept in accordance with specific criteria. The document format is a general

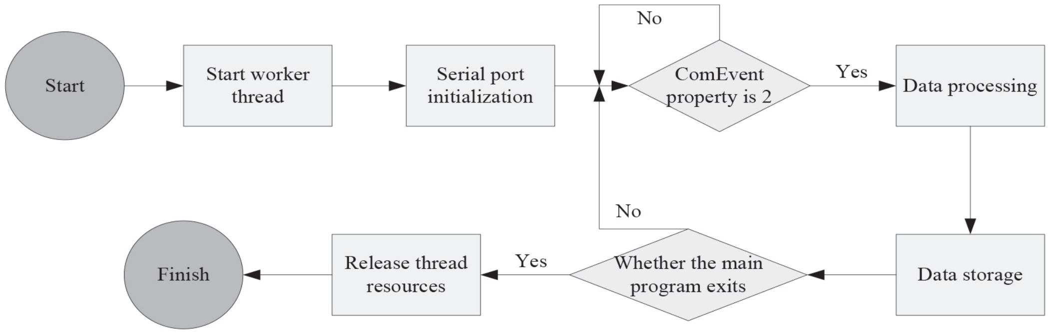

Figure 1 Data collection process.

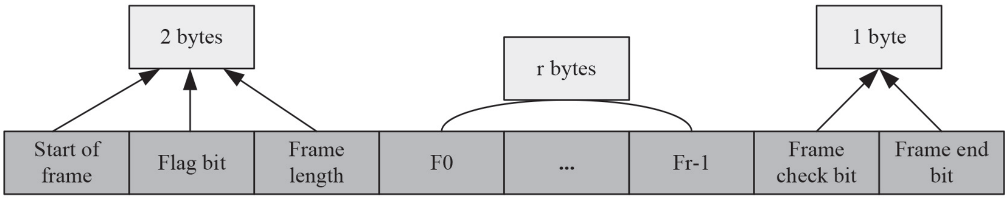

Figure 2 Data frame format.

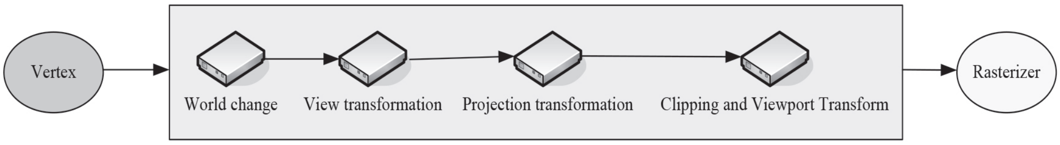

Figure 3 Vertex formation process.

format. The original values of the data gathered by the mobile phone's gyroscope, acceleration sensor, and gravimeter are saved in the system software path's subdirectory after the service platform analyzes it. The data is also saved as an XLS file to make it easier to load and read.

In the Microsoft Foundation Class, the production of the display area is determined by the driving context of environmental equipment engineering. In the APP application software based on Microsoft's basic class library architecture, in order to create a view area, it is necessary to obtain the user area driving context of the current view area, and perform corresponding actual production operations in the driving context. When creating a virtual Direct3D-rendering natural environment in the Microsoft Basic Class View area, it is necessary to make a corresponding link in the driver context. One can first define the Direct3D page to configure the environment. Second, the main parameters of the background cache file bevel construction must be set. The surface structure of the cache file gives the definition, overall width and format, window mode, etc. of the cache file. Finally, a virtual device target is established, and 3D rendering of the scene is performed through this device target [20–21].

The pixel coordinates of the three-dimensional endpoints of the virtual 3D indoor space can be projected onto the screen. As shown in Figure 3, the endpoint formation process requires several steps of world transformation, view transformation projection transformation, clipping and viewport transformation. These are:

(1) Transformation includes the actual operation of the entity model, view and projection. In a simulated 3D scene, the camera is used to take pictures of the virtual machine projected onto the screen [22]. View transformations specify the position and orientation of the 3D camera used to view the 3D scene and form the image that can be seen on the screen. The transformation depends on the method used to project the scene onto the screen and the category of visual effects. There are two main types of projection: orthographic projection and perspective projection. Manipulation of the horizon range must set the horizon size and the aspect ratio of the resulting photo. Orthographic projection mode is generally used in the engineering design industry. Objects are projected onto the screen immediately without the need for pitch transformation, and the relative size of objects does not change. In projection mode, similar to a real-world scene, background scenes are smaller than those in the foreground. Solid model transformations move, rotate, and scale objects in 3D space. The basic purpose is to set and optimize the position and orientation of every object in the scene [23].

(2) The dialog view area marked last is a square area; so, when the scene is rendered in 3D, a part outside the scene is cut off.

(3) Finally, the viewport transformation is performed. That is, the relationship between the transformed plane coordinates and screen pixels is established. The dialog box specifies the area occupied by the photos that make up the scene in the display area of the system software window, which can adjust the position of the photos in the display area of the mobile phone software page

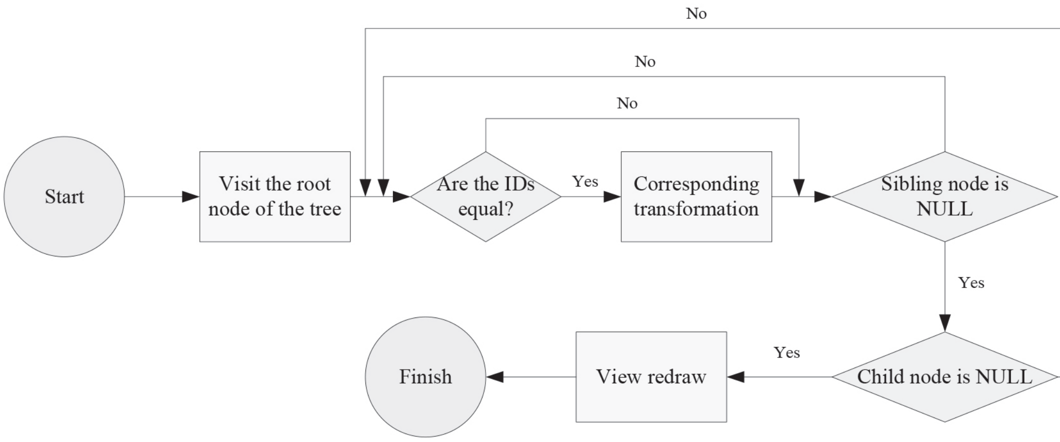

Figure 4 Mannequin-driven process.

by adjusting the dialog box. Therefore, during the reset period of the 3D scene, the corresponding view transformation, projection transformation and viewport transformation need to be equipped in advance.

There is a certain difference between the light intensity of the real world and that of the 3D virtual animation world. In the real world, the human eye perceives clarity by detecting the light photons that are reflected or emitted from the surface of objects and absorbed by the retina. In the 3D virtual animation world, the lighting fixture entity model is used to simulate the lighting fixtures in the real world. This equation of light can be processed extremely quickly via a computer. The lighting effect solid model divides the light source into four separate components: diffuse light, specular light, reflected light, and emitted light (or radiant light), each of which can be turned on and off independently. In the 3D lighting solid model, the material color is indicated by the transmission of the material to the basic red, green, and blue light. The final pixel is the result of multiplying the color of the light and the reflectance of the light by the material. During the scene reset period, the color and location of the light source must be set [24].

The driving of the human body model needs to undergo three-dimensional space transformation, which depends mainly on the 4x4 transformation matrix with one more dimension than that of the real sensory world coordinate system. The purpose of 3D space transformation is to unify the actual operations of scaling, translation and rotation. DirectXSDK defines it as the D3DXMATRIXA16 structure, and the light-load operator performs basic operations such as addition and subtraction of drainage matrix, multiplication and division. The DirectXSDK also creates pages with zooming, panning, and rotating features.

In the human body posture calculation step, the standard quaternion of the coordinate system is derived via the data information posture measurement control module. The 3D scene created in Direct3D is paired with the left-handed coordinate system, so coordinate system transformation from the coordinate system to the display coordinate system is required. If a person wants to achieve the space transformation of the human body model, the pose quaternion must be converted into an indoor space transformation matrix.

Figure 4 shows the mannequin-driven process. The user can browse the root node of the person tree first, and then determine whether the segment IDs are the same. If they are the same, the transformation matrix is multiplied to the left. After that, the sibling nodes of this node can gradually be traversed. If it is not empty, the recursive algorithm is implemented. If it is empty, it traverses the child nodes of this node. If the child node is not empty, it is enabled again. If it is empty, it means that the child nodes and level nodes of the node are empty. Finally, the main view is redrawn and the driving mannequin is complete.

This paper proposes a high-precision motion capture system based on a three-dimensional space animation scene based on an optical fiber communication network. The formulas involved are as follows:

$$H^a = \Phi_H(R^a, H^{a-1}) \tag{1}$$

$H = \{H_1, H_2 \cdots H_H\}$-human skeleton

$$G^a = \Phi_G(R^a, H^a, G^{a-1}) \tag{2}$$

$G = \{G_1, G_2 \cdots G_G\}$-articulation point

$$T^a = \Phi_T(R^{a-1}, R^a, H^{a-1}, H^a, T^{a-1}) \tag{3}$$

$T = \{T_1, T_2 \cdots T_T\}$-correlation of H and G in fiber network across time domain, feature detection of R-RMPE network

$$H_x = \frac{1}{D}\left\{\sum_x^D \left[f_{l,s} - f_{l,d} + l\right]_+\right\} \tag{4}$$

The characteristic Euclidean distance corresponding to the two samples $f_{l,s}$ and $f_{l,d}$-

$$f_{l,s} = |p(U_{x,y}) - p(U_{x,y-1})|^2 \tag{5}$$

$p(U_{x,y-1})$, $p(U_{x,y})$-encode the features of the picture

$$f_{l,d} = |p(U_{x,y}) - p(U_r)|^2 \tag{6}$$

$p(U_r)$-encode the features of the picture

$$f_y = \sum_{a=1}^{g} ||g_{q_{x=1,y}} - g_{q_{a,r}}|| \tag{7}$$

f_y-Euclidean distance of joint points

$$h_g = u_t - u_a = Q_E \tag{8}$$

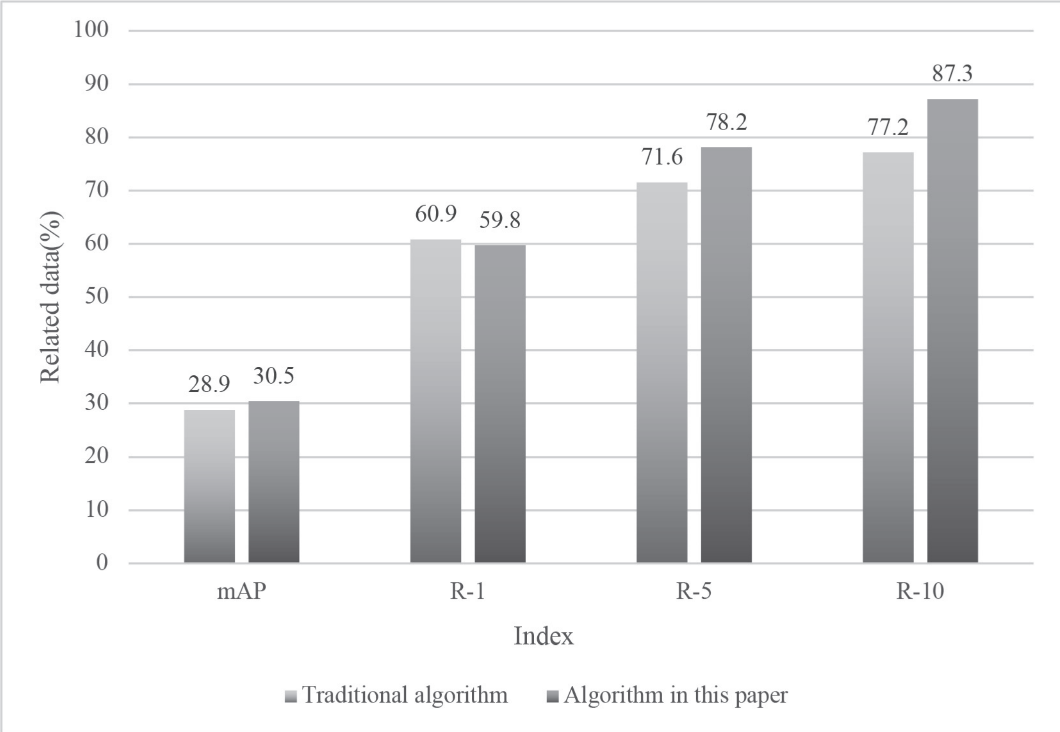

Figure 5 Re-identification performance comparison.

h_g-bone vector, $Q \in T^{3\times d}$-3D pose

$$= (0, \ldots, 0, 1, 0, \ldots, 0, -1, 0, \ldots 0)^A \tag{9}$$

$$O^{h+1} = ||_{f=1}^{F_{h+1}} \propto (\underset{\sigma}{\longrightarrow}_f O^{(h)}\theta_x(Z_f \odot J)) \tag{10}$$

$$O^{h+1} = \propto (MO^{(h)}\theta_x(Z \odot J)) \tag{11}$$

M-transition matrix, $\underset{\sigma_f}{\longrightarrow}$-M is the fth row of M

$$H_u = \sum_{a}^{A}\sum_{x=1}^{Z} ||\widehat{\Phi}_{a,x} - \Phi_{a,x}||_2^2 \tag{12}$$

$\widehat{\Phi}_{a,x}$, $\Phi_{a,x}$-predicted and true joint coordinates, H_u-3D joint point prediction loss

$$H_n = \sum_{a=1}^{A}\sum_{n} ||\hat{N}_{a,x} - N_{a,x}||_2^2 \tag{13}$$

$\hat{N}_{a,x}$-predicted bone length, $N_{a,x}$- Standard bone length

3. EXPERIMENTAL ANALYSIS OF HIGH-PRECISION MOTION CAPTURE SYSTEM

To examine the performance of our proposed high-precision capture system, we conducted an experimental analysis of the capture system. Its key software development tools were run on free and open-source software computer operating systems and web server appliances; the application server has eight NVIDIA RTX2060 discrete graphics cards. The relevant results obtained from the experiments are as follows:

The experiments involved fusing joint point metrics with human airspace attributes. The effectiveness of the developed airspace feature + joint point measurement was tested against a conventional re-identification model. The evaluation dataset was taken from a subset of the Market1501 dataset.

Figure 5 shows the re-identification performance comparison diagram. It can be seen that the confidence ranking is calculated in the search database. The re-identification performance captured by the traditional method has a probability of 60.9% of the correct result in an action with the highest confidence, which is slightly higher than the 59.8% of the method proposed in this paper. The chance of accurate motion capture findings using the method described in this work likewise steadily increases as the number of motion statistics with the greatest confidence multiplies. The difference eventually widens, making it substantially more expensive than the conventional approach. When using the method proposed in this paper to search the action library, the percentage of accurate results for the top 10 actions with the highest confidence is 87.3%, compared to just 77.2% when using the traditional method. The strategy proposed in this paper outperforms the conventional method by 10.1%. According to the average precision of the entire class, the method described in this paper has a higher average precision than the conventional method.

Whether it is an estimation of pose or motion capture, accuracy is only one measure of performance. Another important metric is the actual processing speed. Therefore, the processing speed performance test is carried out in this study. Figure 6 shows the comparison of the prediction accuracy of the new algorithm and the conventional algorithm for various input frame rates, both obtained with the mAP protocol. As can be observed, the prediction accuracy increases along

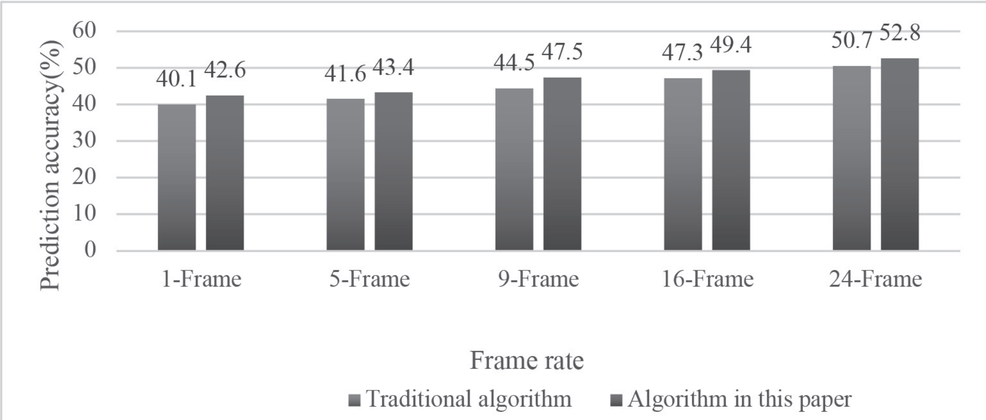

Figure 6 Comparison of prediction accuracy of different input frame rates using the mAP protocol.

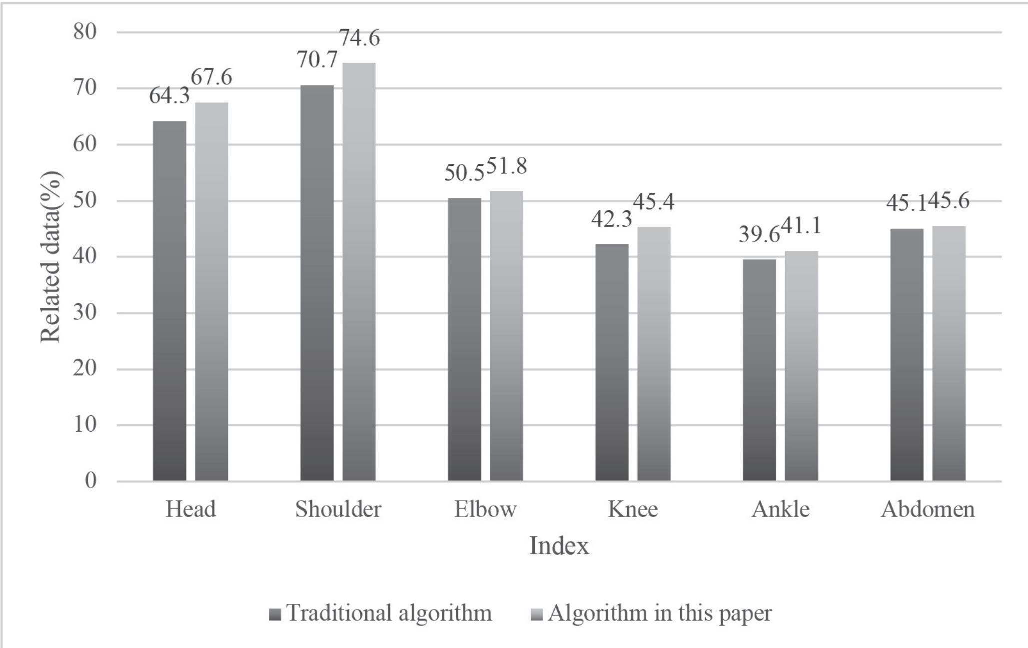

Figure 7 Accuracy comparison of some joint points on MPII dataset.

with the constant improvement of the input frame rate. The experimental findings indicate a 9-frame input frame rate. The forecast accuracy of the method used in this research differs from the conventional method by 3%. The improvement in forecast accuracy is currently at its maximum level.

As shown in Figure 7, the accuracy of some joint points on the MPII dataset is compared. It is evident that the method described in this research produces a superior joint point capture effect than does the conventional method. The best among them is the motion capture's impact on the shoulder. The method described in this work has a shoulder capture accuracy of 74.6%, making it more accurate than the conventional method. Following that, the precision of the capture of the head, elbow, abdomen, knee, and ankle follows sequentially. In order to identify more effective ways to increase capture accuracy, future research should investigate the capture accuracy of the elbow and abdomen. The capture accuracy for these joints is not significantly higher than that of the traditional approach.

Figure 8 shows the change trajectory of joint points in the time domain. It can be seen that the traditional method does not add the fiber high-speed time domain, and the distance between the captured joint point and the center has been beating up and down the real value, and there are many errors with the real value, and only a few parts coincide with the real value.

After this study uses the optical fiber communication network technology, the addition of the high-speed time domain of the optical fiber makes the distance between the captured joint point and the center more closely approximate the real value, the amplitude of the up and down jump is significantly reduced, and the entire curve is smoother. Therefore, the addition of the optical fiber high-speed time domain also improves the estimation accuracy of the joint points. Figure 9 shows the average performance comparison between time domain and no time domain data. It can be seen that when there is no high-speed optical fiber time domain, the average accuracy of motion capture is 46.7%. The addition

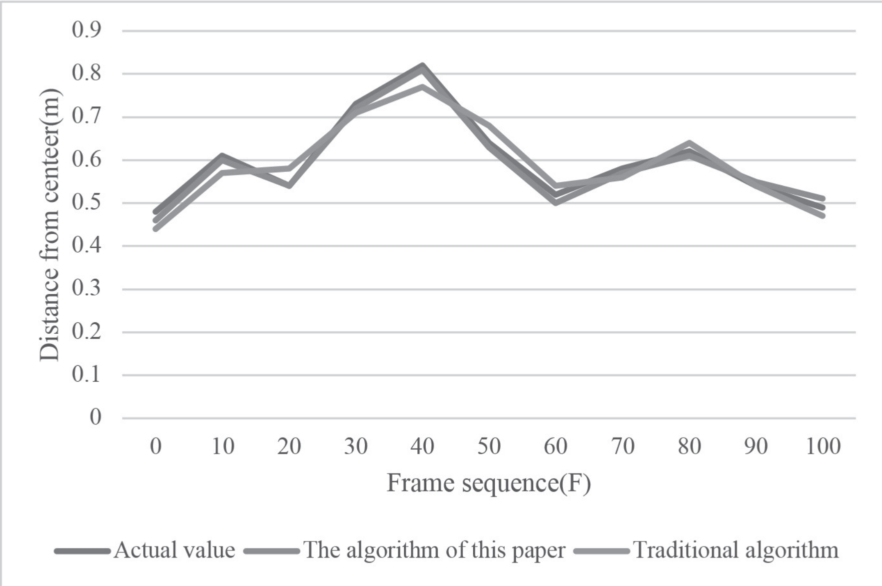

Figure 8 Change trajectory of joint points in time domain.

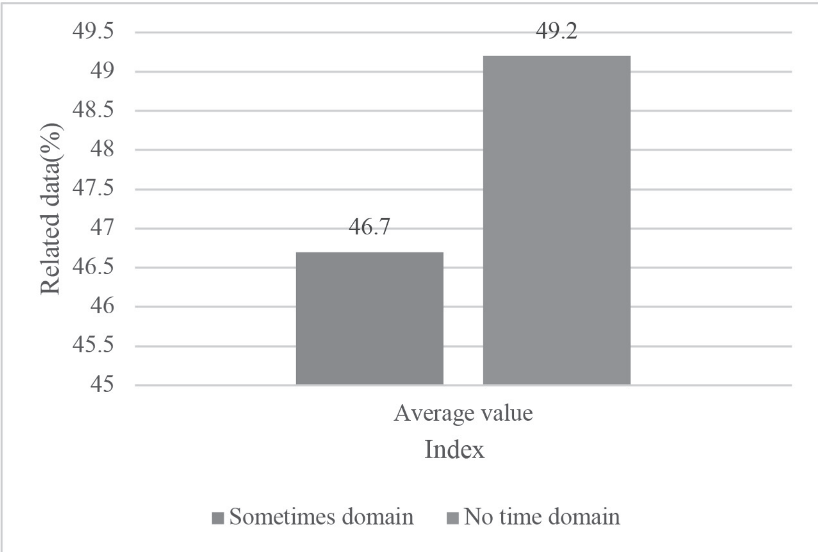

Figure 9 Average performance comparison between time domain and no time domain information.

of high-speed optical fiber time domain improves the average capture accuracy of motion capture by 2.5%.

4. CONCLUSIONS

This study was conducted to investigate the inertial sensor human motion capture system software. A high-precision motion capture system was proposed, based on the optical fiber communication network three-dimensional space animation scene construction. VC++ was selected as the software development environment as it integrates the Microsoft basic class library architecture and the multimedia programming interface user interface library, and loads and promotes the mani kin in the virtual three-dimensional scene. Real-time attitude computation, data collection and storage, as well as real-time human movements, have all been combined into a multipurpose integrated management platform, and appropriate accuracy tests were conducted. The detection results demonstrate that this method's capture accuracy is superior to that of the conventional method. Moreover, this study has produced an attractive UI page for the mobile phone software in addition to completing the software development of human motion posture capture, real-time motion capture, and 3D reconstruction features.

REFERENCES

1. Yang B, Dong H, Saddik A E. Development of a Self-Calibrated Motion Capture System by Nonlinear Trilateration of Multiple Kinects v2. IEEE Sensors Journal, 2017, 17(8):2481–2491.
2. Ganguly A, Rashidi G, Mombaur K. Comparison of the Performance of the Leap Motion Controller TM with a Standard Marker-Based Motion Capture System. Sensors, 2021, 21(5):1750–1750.

3. Schlage Nananana. Development of a mobile, cost-effective and easy to use inertial motion capture system for monitoring in rehabilitation applications. Current Directions in Biomedical Engineering, 2021, 7(2):586–589.
4. Mrozek A, Sopa M, Myszkowski J. Assessment of the Functional Movement Screen Test With the Use of Motion Capture System by the Example of Trunk Stability Push-Up Exercise Among Adolescent Female Football Players. Vibrations in Physical Systems, 2020, 31(2):2020220–2020220.
5. Khaliq, Z., Khan, D. A., Baba, A. I., Ali, S., & Farooq, S. U. (2024). Model-based framework for exploiting sensors of IoT devices using a botnet: a case study with android. Cyber-Physical Systems, 11(1), 1–46.
6. Mostashiri N, Dhupia J S, Verl A W. A Novel Spatial Mandibular Motion-Capture System Based on Planar Fiducial Markers. Sensors Journal, IEEE, 2018, 18(24):10096–10104.
7. Burger B, Puupponen A, Jantunen T. Synchronizing eye tracking and optical motion capture: How to bring them together. Journal of Eye Movement Research, 2018, 11(2): 5–5.
8. Gn A, Rmk A. Motion capture system validation with surveying techniques. Materials Today: Proceedings, 2018, 5(13): 26501–26506.
9. Napoli A, Glass S, Ward C. Performance analysis of a generalized motion capture system using Microsoft Kinect 2.0. Biomedical Signal Processing and Control, 2017, 38(Sep.):265–280.
10. Zhang T. Design of Virtual Reality Visualization Display System Based on Big Data Technology. Engineering Intelligent Systems, 2024, vol. 32 no. 3, pp. 225–233.
11. Bleser G, Taetz B, Miezal M. Development of an Inertial Motion Capture System for Clinical Application. i-com, 2017, 16(2):113–129.
12. Baskwill A J, Belli P, Kelleher L. Evaluation of a Gait Assessment Module Using 3D Motion Capture Technology. International Journal of Therapeutic Massage & Bodywork Research Education & Practice, 2017, 10(1): 3–9.
13. Armitano-Lago C, Chaaban C, Cain M S. Multi-Camera Portable Markerless Motion Capture System Accurately Captures Lower Limb Kinematics During Functional Tasks: 529. Medicine & Science in Sports & Exercise, 2021, 53(8S): 176–176.
14. Tsilomitrou O, Gkountas K, Evangeliou N. Wireless Motion Capture System for Upper Limb Rehabilitation. Applied System Innovation, 2021, 4(1): 14–14.
15. Yang, J., Li, X., Liu, W., Shao, H., & Li, G. (2025). Research on Recognition Method of Non-Legacy Dance Action Based on Multi-Feature Fusion. International Journal of Intelligent Information Technologies (IJIIT), 21(1), 1–16.
16. Kb A, Jc B, Ldm C. Concurrent validity and within-session reliability of gait kinematics measured using an inertial motion capture system with repeated calibration. Journal of Bodywork and Movement Therapies, 2020, 24(4):251–260.
17. Tong L, Liu R, Peng L. LSTM-Based Lower Limbs Motion Reconstruction Using Low-Dimensional Input of Inertial Motion Capture System. IEEE Sensors Journal, 2020, 20(7):3667–3677.
18. Ligorio G, Bergamini E, Truppa L. A Wearable Magnetometer-Free Motion Capture System: Innovative Solutions for Real-World Applications. IEEE Sensors Journal, 2020, 20(15): 8844–8857.
19. AM Gomez-Blasco, A Hernandez-Fernandez, Roche-Albero A. Results measured by means of a motion capture system in proximal humerus fractures treated by osteosynthesis with locking plate. Revista Espanola de Cirugia Ortopedica y Traumatologia, 2019, 63(4):268–274.
20. Maruyama T, Tada M, Toda H. Riding Motion Capture System Using Inertial Measurement Units with Contact Constraints. International journal of automation technology, 2019, 13(4): 506–516.
21. Hwang J, Hwang S. Effect of External Load on Shoulder Joint Active Relocation Using 3D Motion Capture System: A Pilot Study. Physical Therapy Korea, 2018, 25(2):71–77.
22. Jiang F. Animation Design System Based on 3D Image Technology. Engineering intelligent Systems, 2024, vol. 32 no. 5, pp. 411–419.
23. Kitzig A, Demmer J, Bolten T. An HMM-based averaging approach for creating mean motion data from a full-body Motion Capture system to support the development of a biomechanical model. Current Directions in Biomedical Engineering, 2018, 4(1):389–393.
24. Secco E L, Maereg A T, Reid D. 1 An Integrated Haptic System combining VR, a Markerless Motion Capture System & Tactile Actuators. ICST Transactions on Ambient Systems, 2018, 5(17):154375–154375.

Jiayi Li was born in Zibo, Shandong, P.R. China, in 1986. She received the bachelor's degree and master's degree from Shandong University of Technology, P.R. China. She received her PhD from Gachon University, Korea. At present, she works in School of Department of Anime Arts, Zibo Polytechnic University. Her research interests include anime arts.
Email: 12660@zbvc.edu.cn